University of Dayton
Office of Technology Partnerships
937.229.3469

LITHIUM-AIR CELLS INCORPORATING SOLID ELECTROLYTES HAVING ENHANCED IONIC TRANSPORT AND CATALYTIC ACTIVITY

Case #: UD-494

US Patent Pending; Publication # 20090317724

Inventor: Binod Kumar, et. al.

Designing Ionic Conductors and Electrochemical Devices Based on the Space Charge Effect

Abstract:

Electrochemical devices such as batteries, fuel cells and sensors use an ionic conductor as an electrolyte normally placed between the electrodes. The electrolyte could be a liquid or solid. Liquids have been preferred in commercial electrochemical devices because they exhibit high conductivity ($10^{-3} – 10^{-1}$ Scm^{-1}) around the operating temperature. The high conductivity of liquids allows superior performance of a device employing them. The solids are generally associated with lower conductivity and therefore they are of lesser interest from the commercial application point of view. There are a number of different approaches which can be employed to enhance the conductivity of solids. Prominent among them is to develop a proper crystal structure so as to create a path for the transport of conducting ions. Ceramic ionic conductors based on a $LiTi_2(PO_4)_3$ (LTP) structure create such a path. In recent years (1,2) high conductivity solid electrolytes have been developed in materials such as $Li_{1+x}Al_xTi_{2-x}(PO_4)_3$ and $Li_{1+x}Ge_xTi_{2-x}(PO_4)_3$. These ionic conductors have shown high conductivity ($\sim 10^{-3}$ Scm^{-1}) around room temperature, yet they are not as conductive as liquid electrolytes. This patent disclosure presents and explains a technique to further enhance conductivity of these ceramic ionic conductors – exceeding 10^{-2} Scm^{-1} at room temperature. The technique is based on the creation of the space charge in bulk solids.

Description of the Invention:

1. Ionic Conduction and Electrochemical Devices

In an electrochemical device oxidation and reduction of chemical species are spatially separated by an ionic conductor called electrolyte. In the device the electrochemical oxidation of species, such as hydrogen and lithium, is carried out at anode generating electrons and

corresponding ionic species H^+ and Li^+. Such a device is schematically shown in Figure 1. These ionic species travel through the cell internally, i.e., from the anode through the electrolyte to the cathode. The reduction of the ionic species leads to the formation of products such as H_2O and Li_2O. These two basic reactions are the foundations of proton exchange membrane fuel cell (PEMFC) and lithium batteries, respectively.

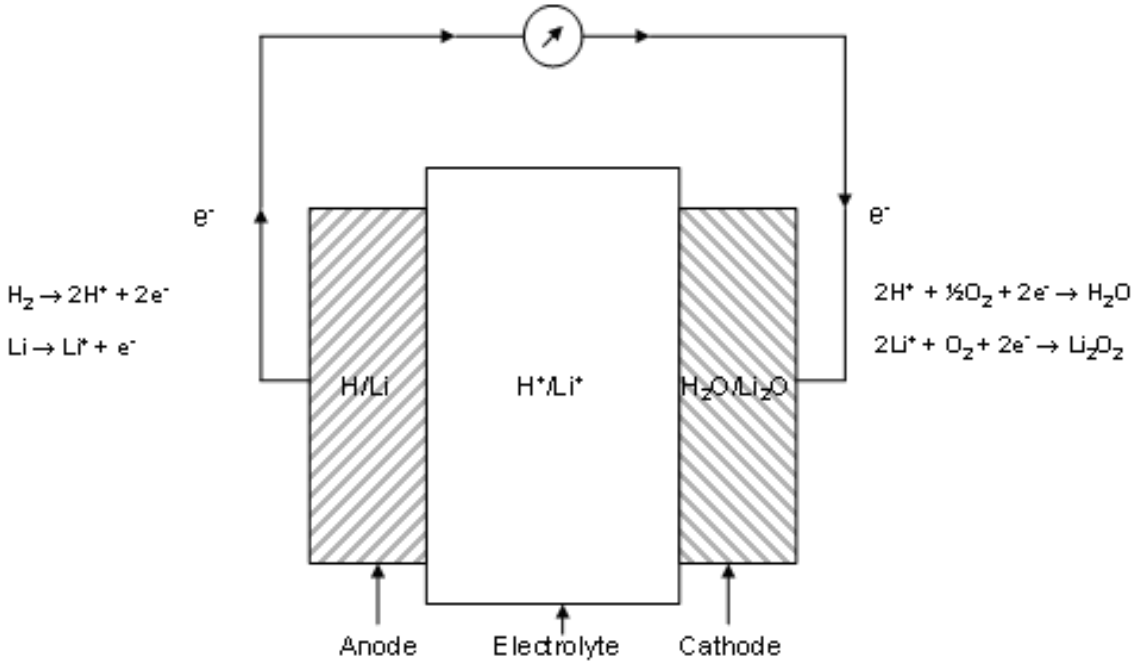

Figure 1. Schematic of an electrochemical device showing the anode, electrolyte, cathode and flow of ions and electrons.

The materials for transporting electrons through the external circuit are numerous, inexpensive metals. However, the materials to transport ions internally are rare and expensive because the mechanisms and requirements of ionic transport are very different from those of the electronic transport.

2. The Space Charge Effect on Ionic Conductivity

A solid ionic conductor consists of a significant concentration of free ions which are in random motion and vibrations. The amplitude of the vibrations increases with increasing temperature. An application of an electric field leads to a long-range transport of the conducting ions. The physical presence of the conducting ions is shown by arrows in Figure 2(A). When a dielectric phase is dispersed in a homogeneous ionic conductor of the type shown in Figure 2(A), an interaction between the conducting ion and the dielectric phase takes place leading to immobilization of some of the free ions. The interaction is graphically shown in Figure 2(B). Once some of the free ions are immobilized they create a localized field which influences transport of the remaining free ions. In some cases, the conductivity could be enhanced by orders of magnitude due to the creation of the space charge within the bulk structure of the heterogeneous electrolyte.

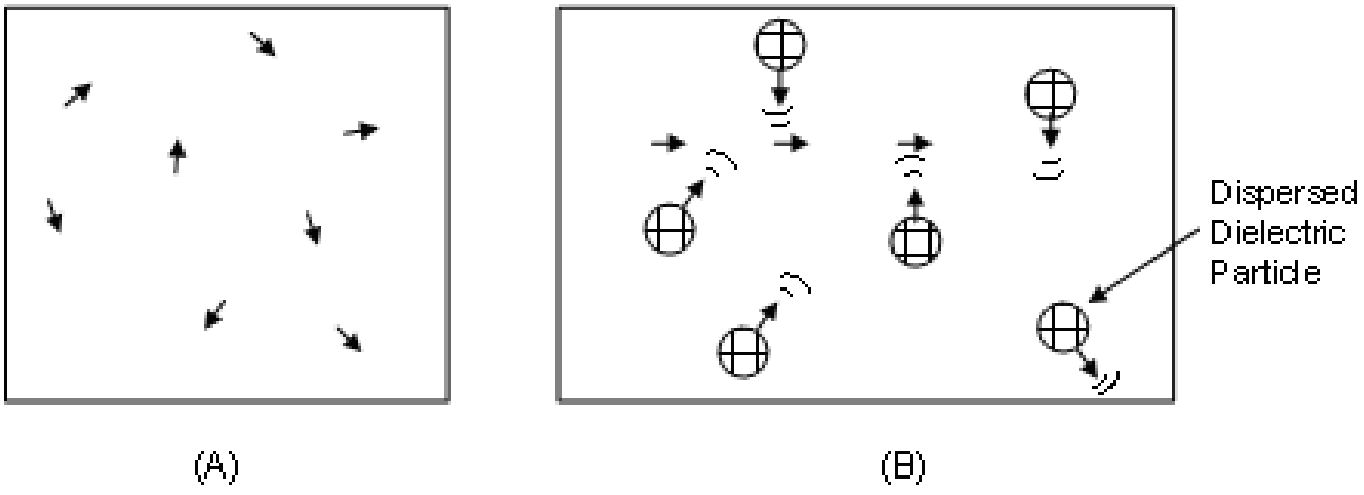

Figure 2. Nanoscopic view of (a) homogeneous ionic conductor and (b) heterogeneous ionic conductor.

3. The Formation and Destruction of the Space Charge

The creation of a stable space charge effect requires careful consideration of choices with respect to the nature of the matrix and dispersant phase. It is preferred to use single ion conductors as the matrix phase and the dispersant phases with small particle size and a high dielectric constant. These attributes of the two phases lead to an enhanced interaction between them and a stable space charge effect. It should be noted that the interaction as depicted in Figure 2(b) can also be destroyed by the thermal energy. Therefore, the intent of this invention is to create the space charge and retain its effects in the operating temperature region of the electrochemical device.

A typical heterogeneous, solid ionic conductor exhibiting the space charge effect shows the temperature dependence of conductivity data as depicted in Figure 3. The conductivity of a typical solid as a function of temperature shows a trend similar to the one shown by a broken line in Figure 3. The existence of the space charge effect increases the conductivity up to the critical temperature (T_C) and then the conductivity shows a precipitous decline at the T_C. If the dielectric phase is represented by D, an interaction as shown by equation (1) takes place below T_C. The interaction leads to the formation of a complex $D:H^+/Li^+$. At the T_C, reaction (1) proceeds towards the left and the space charge is destroyed, leading to the elimination of its effect on the ionic transport.

$$D + H^+/Li^+ \Leftrightarrow D:H^+/Li^+ \qquad (1)$$

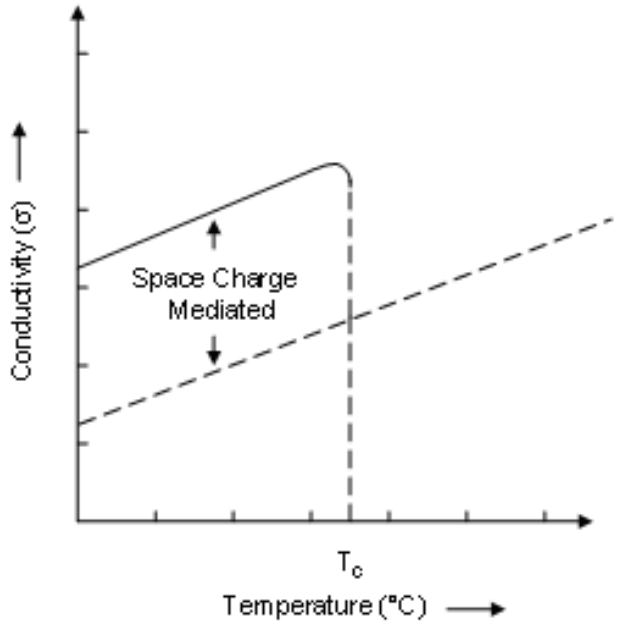

Figure 3. A schematic of the space charge mediated conduction in heterogeneous solids.

Examples

Example 1: Lithium Aluminum Germanium Phosphate (LAGP) Glass-Ceramic

The LAGP glass-ceramic is a derivative of lithium germanium phosphate , $LiGe_2(PO_4)_3$ (LGP). The LGP material exhibits low conductivity ($\sim 10^{-8}$ Scm^{-1}) around the ambient temperature (3). Partial substitution of Ge by Al leads to a charge imbalance and an excess of lithium must be introduced to maintain electrical neutrality. The substitution leads to a major improvement in conductivity ($\sim 10^{-3}$ Scm^{-1}) at ambient temperature such as in $Li_{1+x}Al_xGe_{2-x}(PO_4)_3$ for ~ 0.5 (3). The conductive $Li_{1+x}Al_xGe_{2-x}(PO_4)_3$ phase possesses the rhombohedral structure (space group $R\bar{3}C$) with an open three-dimensional framework of GeO_6 octahedra sharing all corners with PO_4 tetrahedra. The lithium ion resides and migrates through a tunnel contained in the framework. There are two different sites available for Li^+ ions: A_1 and A_2. In the $Li_{1+x}Al_xGe_{2-x}(PO_4)_3$, A_1 sites are fully occupied, whereas A_2 sites are partially filled.

Table 1 shows the molar compositions of two LAGP glass-ceramic specimens identified as LAGP-1 and LAGP-2. LAGP-1 represents the $Li_{1+x}Al_xGe_{2-x}(PO_4)_3$ (x = 0.5) stoichiometry, whereas the LAGP-2 contains an excess of Li_2O that allows the precipitation of the Li_2O phase during crystallization of the LAGP-2 specimen. The Li_2O is the phase which is capable of creating the space charge effect. The conductivity data of the LAGP-1 and LAGP-2 are shown in Figure 4. The LAGP-2 specimen shows higher conductivity, by about a factor of three, in the entire temperature range of -40 to 145°C in spite of having similar energy of activation, E_a. The enhanced conductivity is attributed to the presence of excess Li_2O. The Li_2O is a polar molecule which is believed to form a complex $Li_2O{:}Li^+$ as expressed by equation (2). The $Li_2O{:}Li^+$ complex becomes a source of a localized electric field which enhances transport of the remaining Li^+ ions. The effect is also illustrated in Figure 2(b). Figure 4 also shows an inflection in the Arrhenius plot at about 70°C. The inflection is attributed to the precipitation and existence of $AlPO_4$ in both of the specimens.

$$Li_2O + Li^+ \Leftrightarrow Li_2O{:}Li^+ \qquad (2)$$

Table 1. Molar Compositions of Lithium Aluminum Germanium Glass-Ceramics

	LAGP-1	LAGP-2
Li_2O	18.75	19.75
Al_2O_3	6.25	6.17
GeO_2	37.50	37.04
P_2O_5	37.50	37.04

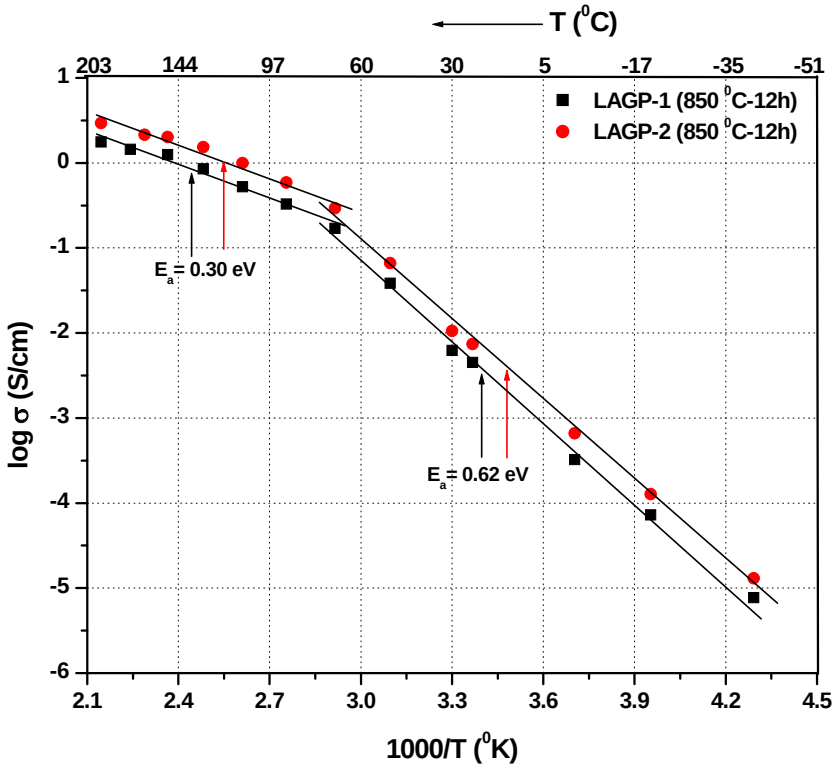

Figure 4. Temperature dependent conductivity of LAGP-1 and LAGP-2 of glass ceramic specimens prepared by crystallizing glass sheets at 800°C for 12 hours.

The $Li_2O{:}Li^+$ complex can be destabilized and the reaction (2) can be forced to proceed in the reverse direction by the thermal energy that can be provided by heating the specimens to higher temperatures. Figure 5 shows the conductivity data of the LAGP-1 and LAGP-2 in the 160 to 500°C temperature range. At lower temperatures, 160 to 400°C, the LAGP-2 specimen exhibits high conductivity; however at 350°C, the conductivity drops almost by a factor of five. The drop is attributed to the breakdown of the $Li_2O{:}Li^+$ complex and progress of the reaction (2) proceeds towards the left.

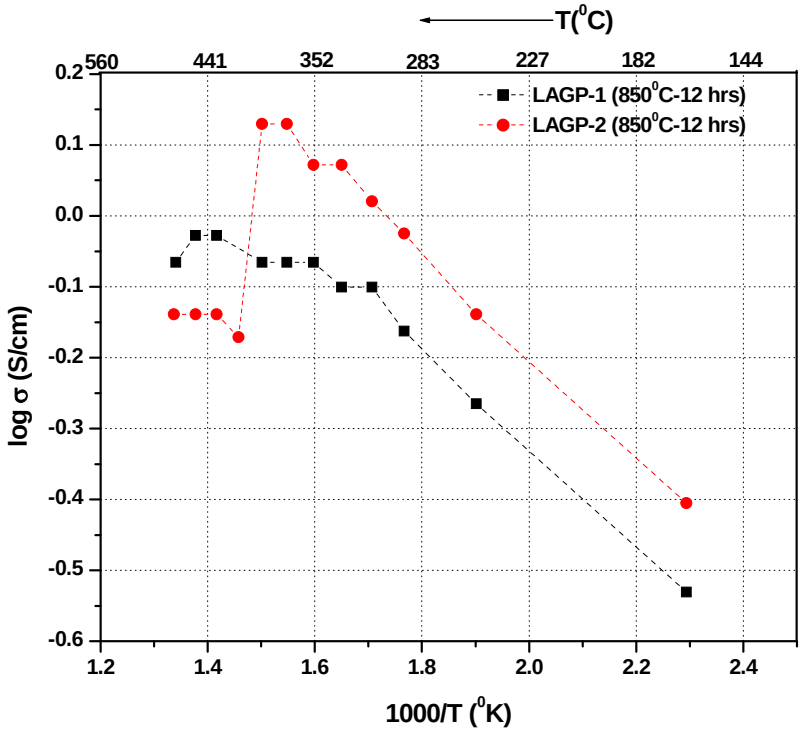

Figure 5. Temperature dependence of conductivity of the LAGP-1 and LAGP-2 specimens in the 160 to 500°C temperature range.

Example 2: PEO:LiBETI (8.5:1)-Li_2O Composite electrolyte

After having shown the beneficial effect of Li_2O in the LAGP glass ceramic specimens, it was also introduced in the polymeric lithium ion conductors based on polyethylene oxide (PEO). The PEO is generally complexed with a lithium salt. In this example the PEO was complexed with LiBETI salt in which various concentrations of Li_2O were introduced. Specimens in the form of films were prepared by energy milling and hot pressing. The conductivity data of these specimens are shown in Figure 6. In these polymer specimens, Li_2O in limited concentrations – about 2 wt% – increases conductivity by almost a factor of five. The space charge induced effect on conductivity due to the presence of Li_2O is evident. Furthermore, since the complex $Li_2O:Li^+$ is stable up to 350°C the higher conductivity electrolytes are expected to remain stable for application in typical polymer lithium batteries.

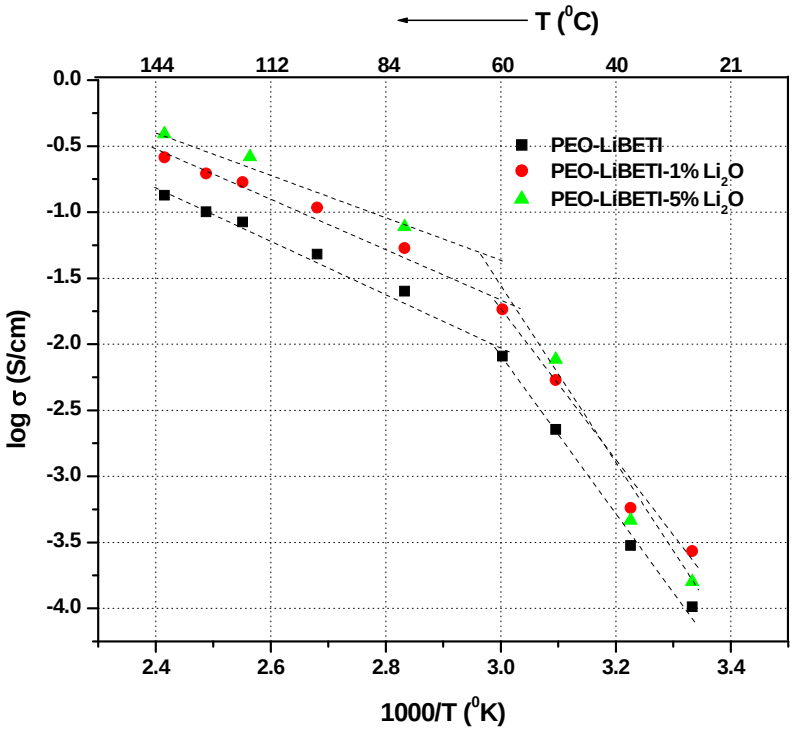

Figure 6. Arrhenius plots of PEO:LiBETI (8:1) with 0, 1, and 5 wt% Li_2O.

Example 3: PEO:LiBETI (8.5:1)-BN Composite Electrolyte

Figure 7 shows conductivity data of PEO:LiBETI (8.5:1) without and with BN nanosize particles as an additive. The concentration of BN was 1 wt%. It is noted that a 1 wt% concentration of BN increased the conductivity in the entire temperature range. In this case the formation of a chemical complex BN:Li^+/$BETI^-$ is also expected which becomes a source of a local electric field that influences the transport of the remaining conducting ions. The thermal decomposition temperature of the BN:Li^+/$BETI^-$ complex is apparently higher as the Arrhenius plot does not indicate any evidence of thermal instability. The PEO degrades rather rapidly at temperatures greater than 150°C. Therefore, no attempt was made to evaluate degradation of the BN:Li^+/$BETI^-$ in these polymer electrolytes.

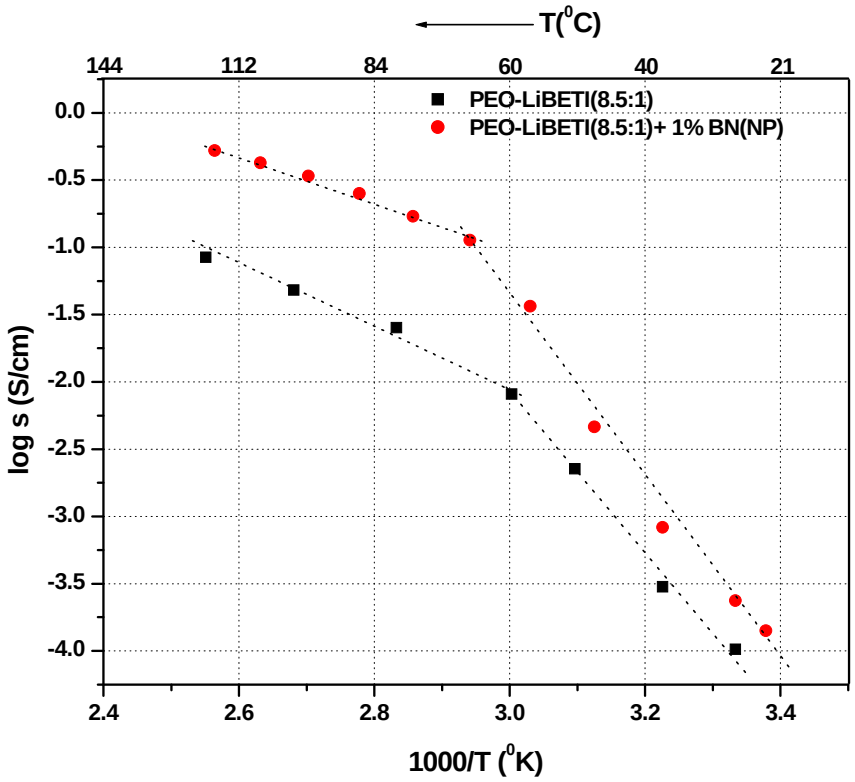

Figure 7. Arrhenius plots of PEO:LiBETI (8.5:1)-BN (1%) composite electrolyte.

The Li-LAGP and Li-PEO:LiBETI(BN)-LAGP laminates were evaluated for interfacial reactions by impedance spectroscopy. Figures 8 (A) and (B) show the impedance data of the laminates. The laminate containing the PEO:LiBETI (1% BN) electrolyte showed lower impedance immediately after their assembly – 740 vs. 6130 Ω , Figure 8(A). The data suggest that the electrolyte lowered the interfacial impedance by a factor of over eight. Even after about 10 days (234 hours), the impedance of the laminate remained lower as compared to the Li-LAGP specimen. Therefore, the Li-PEO:LiBETI (1% BN) is also helpful in improving the interfacial stability between Li and LAGP – a very important consideration in the design of lithium battery.

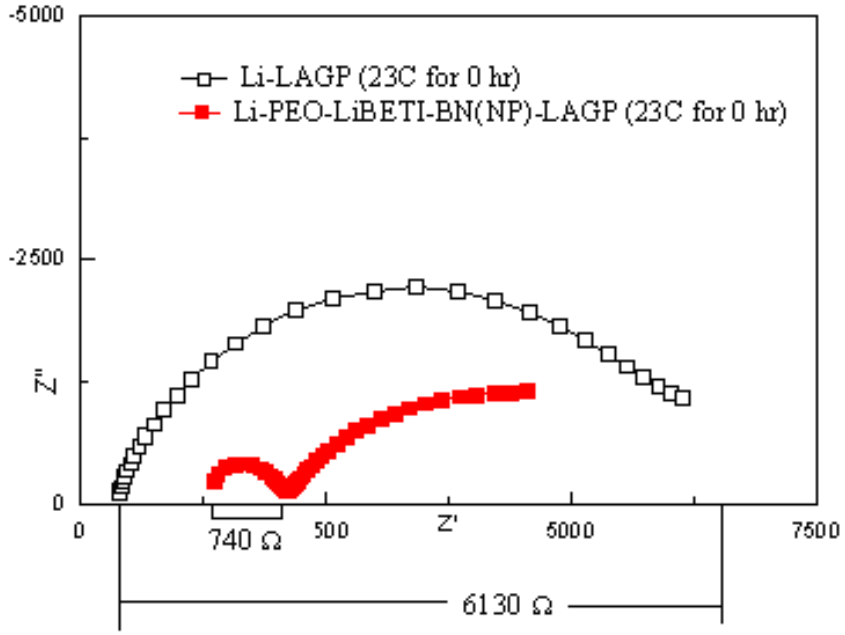

(A)

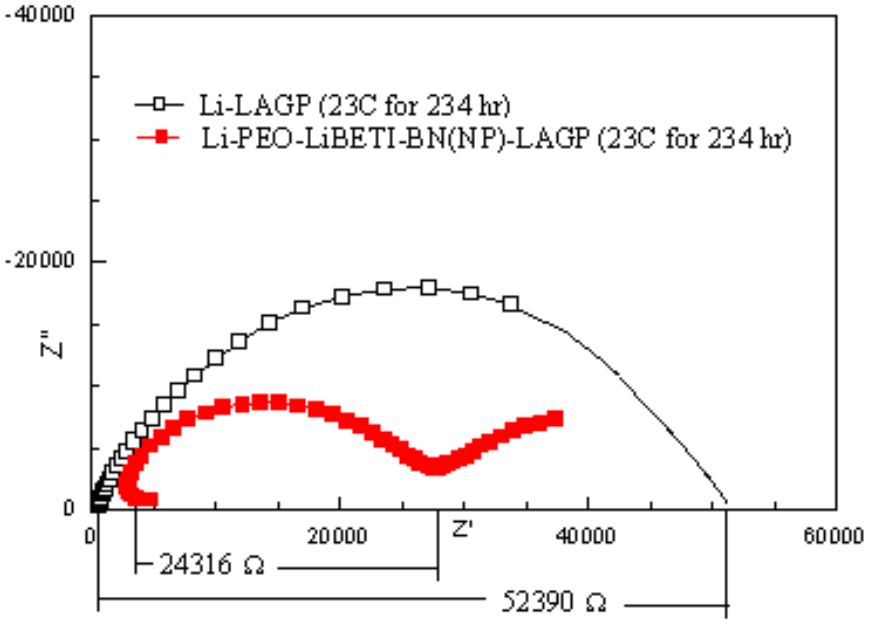

(B)

Figure 8. AC impedance of Li-LAGP and Li-PEO-LiBETI-BN(NP-LAGP) laminates as a function of time; (a) after assembly and (b) 234 hours after assembly.

To investigate thermal degradation of the BN:Li^+ complex, the LAGP electrolyte was doped with BN and conductivity was measured in the 25 to 550°C temperature range. The conductivity data during heating and cooling cycles are shown in Figure 9. During the heating cycle, the conductivity increased rapidly up to about 350°C and then decreased precipitously. During the cooling scan, the conductivity remained lower. From the data provided in Figure 9 it is noted that the BN:Li^+ complex can enhance the conductivity by a factor of five.

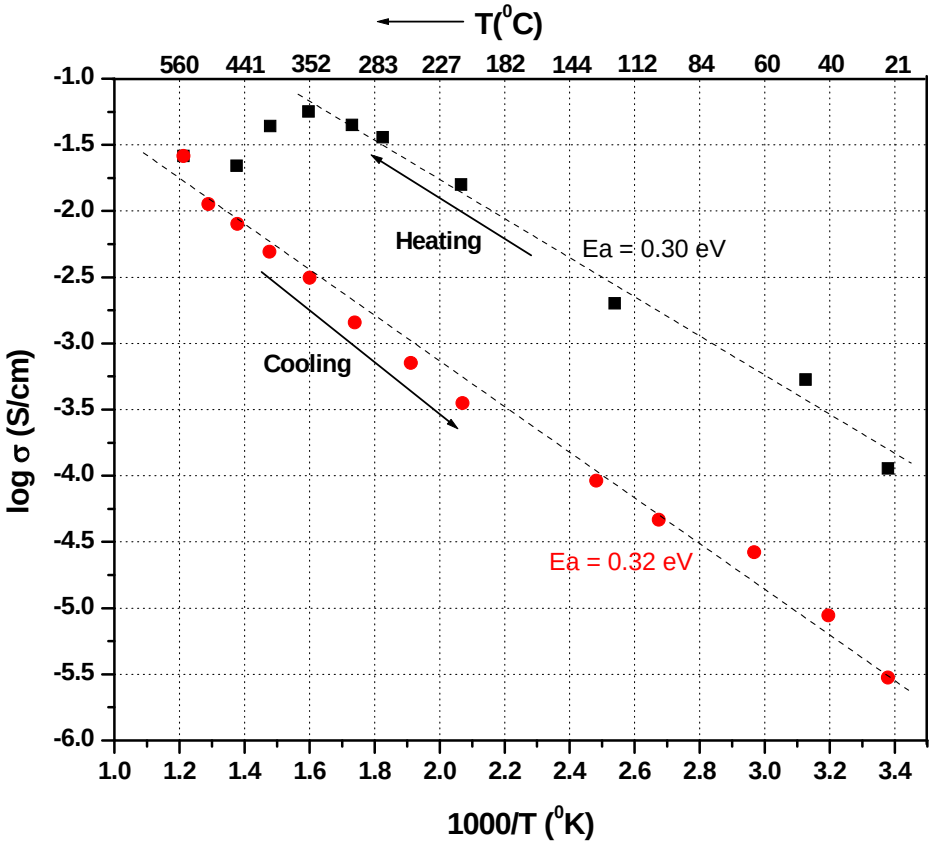

Figure 9. Temperature dependence of conductivity during heating and cooling of LAGP-BN (90:10) specimen sintered at 700°C for 12 hours.

Example 4: Li-O_2/air Cell

A working Li-O_2/air cell was fabricated using ionic conducting membranes developed as described in prior examples. The polymer membranes constituted of PEO:LiBETI (8.5:1)-BN (1 wt%) polymer-ceramic composite electrolyte and LGP membrane constituted of a glass-ceramic with a composition identical to LAGP-2 as shown in Table 1. All these membranes make use of the space charge effect for enhanced ionic conduction. The cathode was prepared using 4Ni5-060 AN Exmet, carbon black (acetylene 50% compressed), LAGP-2 powder, and Teflon (TE-3859). The cell is schematically shown in Figure 10.

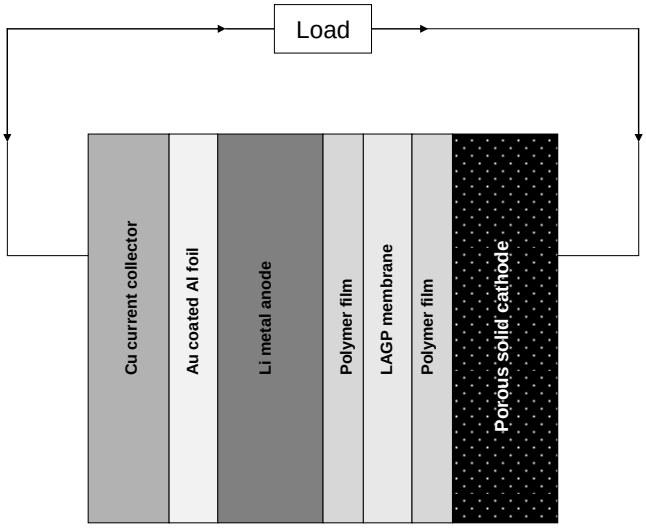

Figure 10. Schematic of lithium-O_2/air cell showing cell components and their arrangements.

The cell exhibiting an open circuit voltage of 3.0V was discharged at 67°C under an oxygen partial pressure of 1 kPa with a current of 0.1 mA. The discharge curve is shown in Figure 11. The cell was subsequently charged with a current of 0.05 mA up to 4.2 V. The discharge and charge capacities were 0.24 mAh and 0.197 mAh, respectively. Prior to this discharge, the cell was cycled 29 times under different conditions.

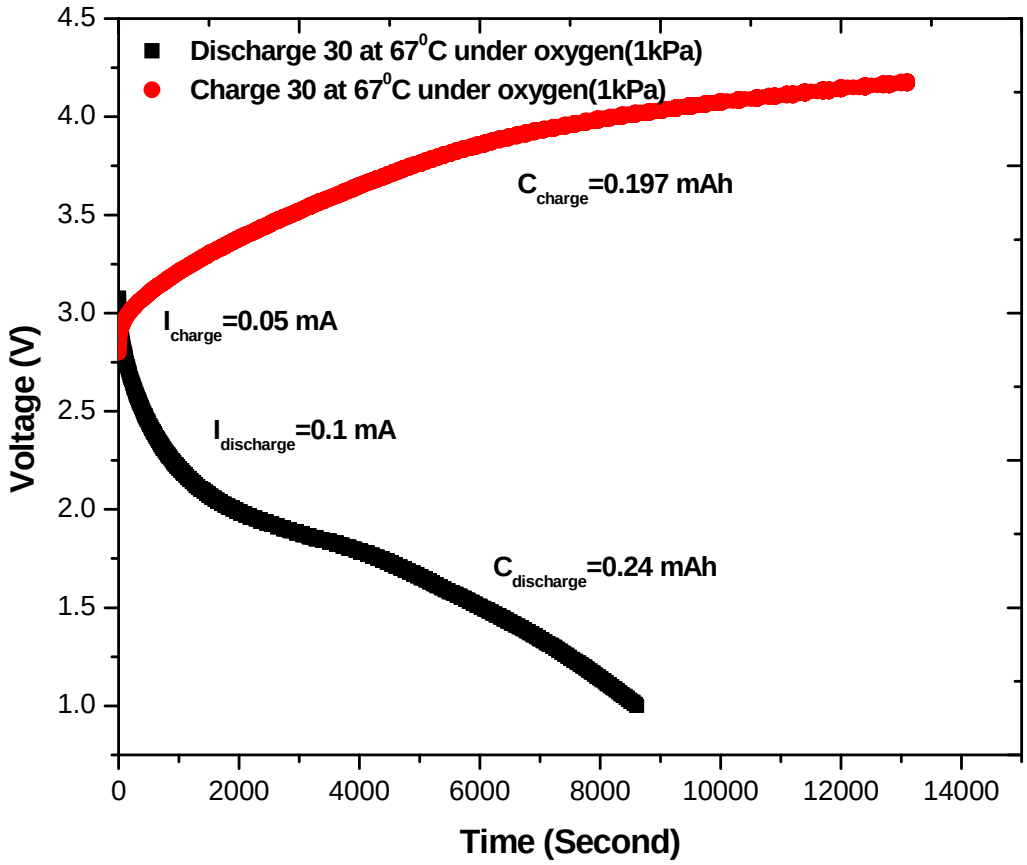

Figure 11. Discharge (30) and charge (30) profiles of a lithium-O_2/air cell.

Figure 12 shows the effect of oxygen partial pressures on discharge capacity at 67°C. Under an oxygen partial pressure of -90 kPa the discharge capacity was 0.21 mAh. The discharge capacity increased to 0.24 and 0.23 mAh under oxygen partial pressures of 2.5 kPa and 100 kPa, respectively. There appears to be a little advantage by increasing oxygen partial pressure beyond 2.5 kPa.

Figure 13 shows temperature dependent discharge capacity under a constant oxygen partial pressure of 1 kPa. The discharge capacity increased from 0.24 mAh to 1.58 mAh by raising the temperature from 67°C to 75°C. Apparently temperature has a major influence on the discharge capacity.

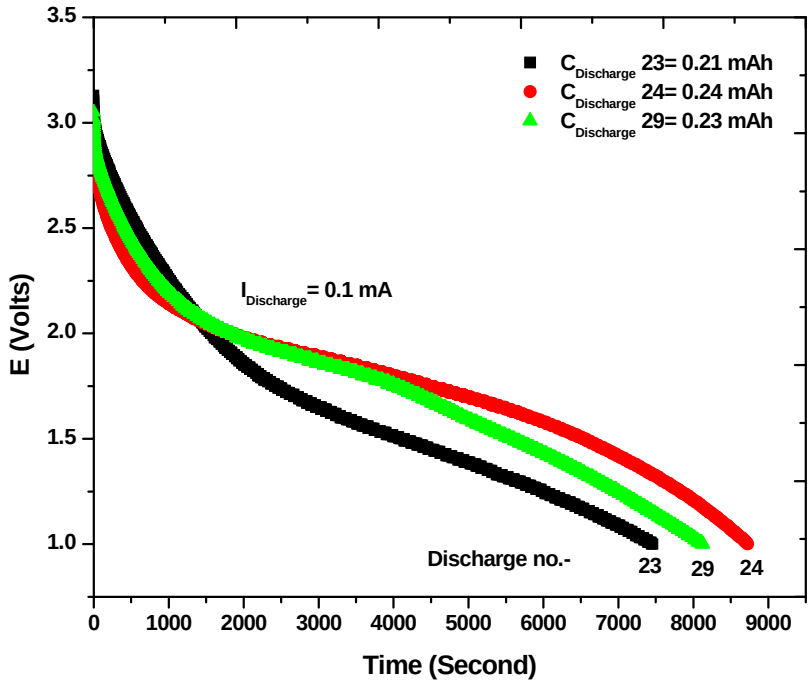

Figure 12. Oxygen pressure dependent discharge capacity of the Li-O_2 cell at 67 ^{0}C for discharge 23 under oxygen (-90kPa), discharge 24 under oxygen (2.5kPa) and discharge 29 under oxygen (100kPa).

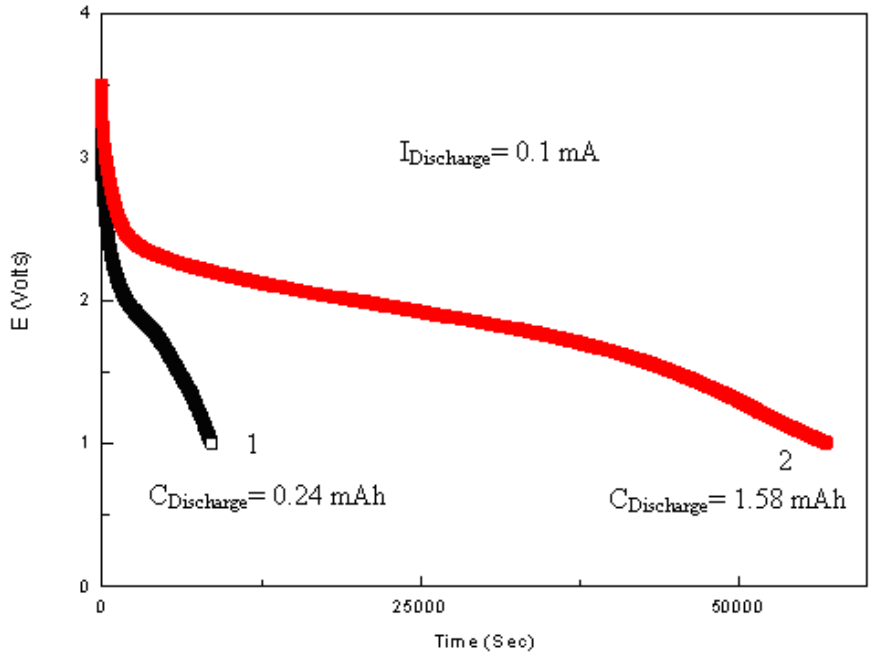

Figure 13. Temperature dependent discharge capacity of the Li-O_2 cell. 1-discharge 30 at 67°C under oxygen (1 kPa) and 2- discharge 32 at 75°C under oxygen (1 kPa).

After stabilizing the cell at 85°C the discharge and charge capacities were measured. The discharge and charge currents were identical, 0.1 mA. The discharge and charge curves are shown in Figure 14. The coulombic efficiency was determined to be 98%. The impedance of the cell during the charge and discharge states were measured and shown in Figure 15. After the charge #s 36 and 37 the cell impedance was 600 and 740Ω, respectively. After discharge the cell impedance increased to 1580 Ω.

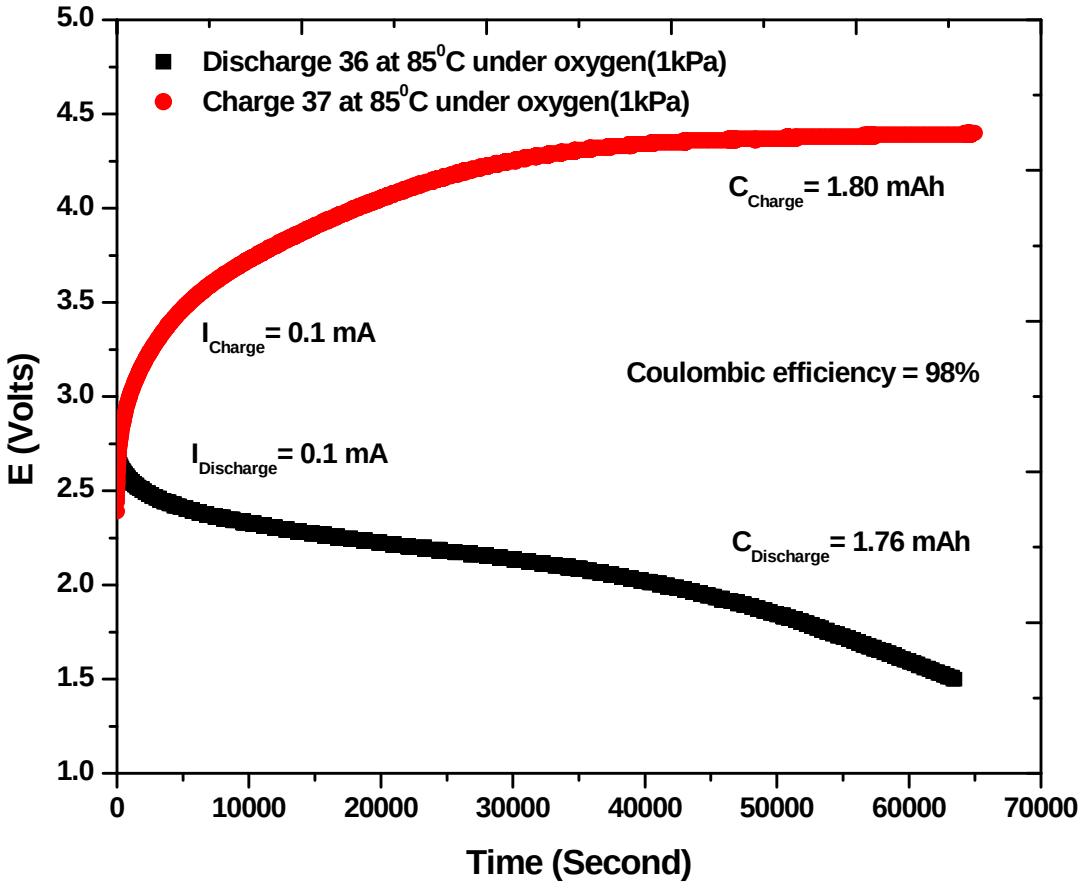

Figure 14. Discharge (36) and charge (37) profiles of a complete rechargeable lithium-O_2/air cell.

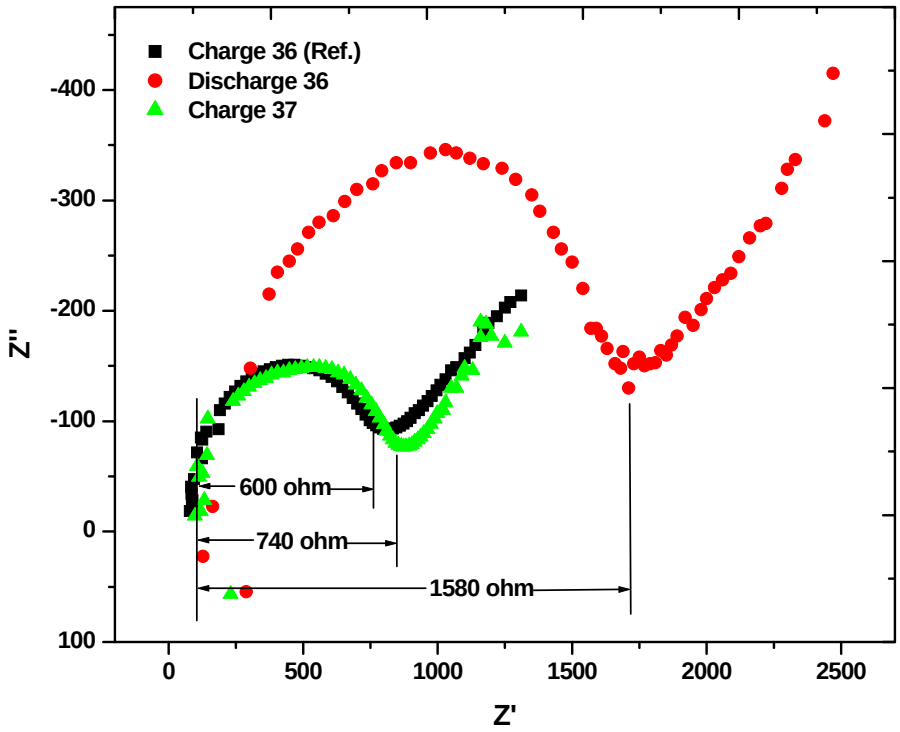

Figure 15. AC impedance spectra of a lithium-O_2/air cell after charge 36 (reference), discharge 36 and charge 37 under oxygen 1 kPa.

References

1. J.S. Thokchom and B. Kumar, "Ionically Conducting Composite Membranes from the Li_2O-Al_2O_3-TiO_2-P_2O_5 Glass-Ceramic, J. Amer. Ceram. Soc. 90(2), 462-466 (2007).
2. J. S. Thokchom and B. Kumar, "Superionic Lithium Conductivity in a Lithium Aluminum Germanium Phosphate Glass-Ceramic," submitted to the J. Electrochem. Soc. for publication.
3. J. Fu, "Fast Li^+ ion conducting glass-ceramics in the system Li_2O-Al_2O_3-GeO_2-P_2O_5," Solid State Ionics 104, 191-194 (1997).